

AD_____

Award Number: W81XWH-11-1-0743

TITLE: Regenerative Medicine for Battlefield Injuries

PRINCIPAL INVESTIGATOR: David L. Stocum

CONTRACTING ORGANIZATION: Indiana University (IUPUI)
INDIANAPOLIS, IN 46202

REPORT DATE: October 2012

TYPE OF REPORT: Annual

PREPARED FOR: U.S. Army Medical Research and Materiel Command
Fort Detrick, Maryland 21702-5012

DISTRIBUTION STATEMENT: Approved for Public Release;
Distribution Unlimited

The views, opinions and/or findings contained in this report are those of the author(s) and should not be construed as an official Department of the Army position, policy or decision unless so designated by other documentation.

REPORT DOCUMENTATION PAGE			<i>Form Approved</i> <i>OMB No. 0704-0188</i>		
Public reporting burden for this collection of information is estimated to average 1 hour per response, including the time for reviewing instructions, searching existing data sources, gathering and maintaining the data needed, and completing and reviewing this collection of information. Send comments regarding this burden estimate or any other aspect of this collection of information, including suggestions for reducing this burden to Department of Defense, Washington Headquarters Services, Directorate for Information Operations and Reports (0704-0188), 1215 Jefferson Davis Highway, Suite 1204, Arlington, VA 22202-4302. Respondents should be aware that notwithstanding any other provision of law, no person shall be subject to any penalty for failing to comply with a collection of information if it does not display a currently valid OMB control number. PLEASE DO NOT RETURN YOUR FORM TO THE ABOVE ADDRESS.					
1. REPORT DATE October 2012		2. REPORT TYPE Annual		3. DATES COVERED 19 October 2011 – 18 October 2012	
4. TITLE AND SUBTITLE Regenerative Medicine for Battlefield Injuries			5a. CONTRACT NUMBER		
			5b. GRANT NUMBER W81XWH-11-1-0743		
			5c. PROGRAM ELEMENT NUMBER		
6. AUTHOR(S) David L. Stocum E-Mail: dstocum@iupui.edu			5d. PROJECT NUMBER		
			5e. TASK NUMBER		
			5f. WORK UNIT NUMBER		
7. PERFORMING ORGANIZATION NAME(S) AND ADDRESS(ES) Indiana University (IUPUI), Indianapolis, Indiana 46202			8. PERFORMING ORGANIZATION REPORT NUMBER		
9. SPONSORING / MONITORING AGENCY NAME(S) AND ADDRESS(ES) U.S. Army Medical Research and Materiel Command Fort Detrick, Maryland 21702-5012			10. SPONSOR/MONITOR'S ACRONYM(S)		
			11. SPONSOR/MONITOR'S REPORT NUMBER(S)		
12. DISTRIBUTION / AVAILABILITY STATEMENT Approved for Public Release; Distribution Unlimited					
13. SUPPLEMENTARY NOTES					
14. ABSTRACT The purpose of this research is to identify the optimum combination of growth factors that stimulate cartilage reeneration across a critical size defect (CSD) in a long bone, using the axolotl, <i>Abystoma mexicanum</i> as a model system. The scope of the research is to characterize fracture repair and determine the length of the CSD in the fibula, use bioinformatics analysis and biochemical analysis of limb proteins to reveal the potential growth factors involved in CSD regeneration, and test these growth factors for their ability to stimulate cartilage regeneration when delivered by a standard pig small intestinal submucosa scaffold (SIS). In year one, we have characterized the response of the fibula to fracture and segment defects of 10, 20, 40 and 50% via X-ray, CT, methylene blue/alizarin red (MB/AR) limn skeleton whole mount staining, and H& E staining of sections at intervals of 15 days, one month, six weeks, two months and three months post-operation. Cartilage formation is detected by H& E staining within one month after fracture and by six weeks with MB stain. The cartilage is mature by 3 months and can be visualized by X-ray and CT. Using the same imaging methods, we determined that the CSD (length at which 50% or more of cases fail to regenerate) is slightly less than 40% of the length of the bone. Because 50% defects fail to regenerate by 3 months in 100% of cases, we will use these defects to test growth factors. We found that a gelatin-coated 8-strand SIS braid releases protein continually for at least 72 hr., indicating that the choice of this scaffold was the right one. Experiments grafting axolotl cartilage and muscle to <i>Xenopus tarsal</i> CSDs indicate that the tissues enhance regeneration, most probably by a paracrine effect; they also enhance regeneration of amputated <i>Xenopus</i> limbs, providing evidence that limb proteins are capable of stimulating regeneration across gaps. Using the Biomap system, we developed pathways and networks of protein interaction using chondrogenesis in fracture repair, cartilage regeneration, and bone regeneration as biological processes to map the literature search. This analysis revealed nine growth factors that have been implicated in fracture repair, only two of which have been tried in segment defect repair. The significance of these results is that we thus now have our starting point to test growth factor combinations to reveal the combination that will yield the most robust regenerative response.					
15. SUBJECT TERMS- Axolotl hindlimb model, fibula, temporal characterization of fracture repair, characterization of repair of 10-50% segment defects, determination of critical size defect (CSD), SIS scaffold, protein release kinetics, bioinformatics analysis of growth factors in fracture repair.					
16. SECURITY CLASSIFICATION OF:			17. LIMITATION OF ABSTRACT	18. NUMBER OF PAGES	19a. NAME OF RESPONSIBLE PERSON
a. REPORT	b. ABSTRACT	c. THIS PAGE			USAMRMC
U	U	U	UU	26	19b. TELEPHONE NUMBER (include area code)

Table of Contents

	<u>Page</u>
Cover Page.....	1
Report Documentation Page.....	2
Table of Contents.....	3
Introduction.....	4
Body.....	4
1. <i>Characterization of Fracture Repair</i>	4
2. <i>Determination of the CSD</i>	5
3. <i>Effects of Scaffolds alone on CSD Repair</i>	7
4. <i>Absorption and Release Kinetics of BSA SIS Scaffolds</i>	8
5. <i>Optimum Technique for Extraction of Limb Proteins</i>	8
6. <i>Axolotl Tissue Grafts Promote CSD and Xenopus Limb Regeneration</i>	8
7. <i>Other Scaffold Types</i>	9
8. <i>In Silico Identification of Growth Factors That Can Potentially Promote CSD Regeneration</i>	9
Key Research Accomplishments.....	14
Reportable Outcomes.....	14
Conclusion.....	14
References.....	15
Appendices.....	16
Supporting Data.....	18

Introduction

The subject of our research is development of the urodele salamander *Ambystoma mexicanum* (axolotl, **Figure 1**) as a model to find the optimum set of growth factors that will enable regeneration of a cartilage template across a CSD in the long bones of the extremities across a critical size defect (CSD). Unlike most models that attempt to regenerate bone directly, with less than optimum filling, regeneration of a cartilage template mimics the initial step of both the normal development of a long bone and fracture repair. The axolotl model can be used to screen single molecules or combinations of molecules for their ability to stimulate regeneration across a CSD. This model has advantages over mammalian CSD models in that there is greater ease of surgical operation and tissue processing, no requirement for bone fixation, and is less expensive to maintain (1). Our purpose is to identify the optimum combination of growth factors that simulate cartilage regeneration across a CSD (and ultimately, the optimum scaffold to deliver these factors). The scope of our research includes defining the CSD for a long bone of the lower leg, the anatomical and histological characterization of cartilage and bone regeneration over defects less than, and equal to or greater than, the CSD, defining protein release characteristics from a standard SIS delivery scaffold, identifying the optimum growth factor combination to be delivered through biochemical analysis of axolotl limb and regeneration blastema protein extracts and by bioinformatic techniques, and testing/verifying the effectiveness of this combination by delivery in the appropriate scaffold.

Body

We report here the research accomplishments during the first year period from September 31, 2011 to October 1, 2012. The objectives to be achieved were to: (1) characterize fracture repair in the fibula of the hind limb and regeneration across a range of defects in the fibula that would allow identification of the CSD, (2) test a standard scaffold for its effect on the CSD, and (3) use an *in silico* approach to identify protein interactions that would reveal key growth factors that might support regeneration across a CSD by attracting cartilage-forming cells (fibroblasts) when delivered by a scaffold.

1. Characterization of Fracture Repair

We examined fracture repair over a two-month time frame in groups of animals by CT imaging, X-ray imaging, whole mount staining for cartilage with the aggrecan-binding stain methylene blue, and H&E staining of longitudinal sections. **Figure 2** illustrates the surgical operation done to fracture the fibula. A longitudinal cut in the skin and muscle is made to expose the fibula and the bone is then cut in the middle, perpendicular to its long axis. **Figure 3** illustrates X-ray photos of fractured fibulae. **Table 1** summarizes the results of fracture repair.

Table 1: Number of cases regenerating cartilage after fracture.

<u>Assessment Method</u>	<u>Time Post-Fracture</u>			
	<u>15d</u>	<u>1 month</u>	<u>6 weeks</u>	<u>2 months</u>
Histology (H&E)	0/6	4/5 (80%)	5/5 (100%)	6/6 (100%)
Methylene Blue	0/6	0/5	4/5 (80%)	6/6 (100%)
Micro-CT	0/6	0/5	0/5	5/6 (83.3%)
X-Ray	0/12	0/10	0/10	10/12 (83.3%)

This data shows that chondrogenesis can be detected in H & E-stained 10 μ sections by one month post-fracture and by 6 weeks in methylene blue-stained whole mounts that detect the aggrecan proteoglycan in cartilage matrix. However, it takes two months for the cartilage to mature to the point where it can be easily visualized by micro CT or X-ray. Thus, chondrogenesis in fractures of the salamander fibula is well underway by one month post-fracture and has fully bridged the fracture gap by two months. **Figure 4** illustrates fracture repair cartilage at two months post-operation.

2. Determination of the CSD

To determine the CSD, the total length of the fibula was first measured from the knee to the tarsal joint (**Figure 5**). We then surgically removed a measured 10%, 20%, 40% or 50% of the length of the fibula (**Figure 6**) and examined the extent of regeneration over a three-month period. H&E staining of sections revealed the initiation of cartilage formation in 10% and 20% defects by 30 days, as in fractures. These defects go on to regenerate cartilage and bone by three months (**Figure 7**).

Two sets of specimens were evaluated for 40% and 50% defects, at 15, 30, 60 and 90 days. The first set at each time point was processed for sectioning and H & E staining. The second set was first subjected to X-ray imaging. This set was then fixed in Bouin's solution and subjected first to micro CT imaging, and second to methylene blue staining for cartilage, followed by staining with alizarin red for bone. The results are summarized in **Tables 2 and 3**.

Table 2: Regeneration across segment defects of 40%. MB/AR indicates that the samples were first stained with methylene blue and photographed, then stained with alizarin red and photographed. In this data set, there were 10 specimens at each time point, except at 3 months where there were 8. All specimens were first imaged by X-ray. Five (2 months) or 4 (3 months) of the 8 specimens were then subjected to micro CT and then MB/AR staining. The remaining 5 or 4 specimens were sectioned for H & E staining.

Assay	40% Segment Defect - 15Day	40% Segment Defect - 1Month	40% Segment Defect - 2Months	40% Segment Defect - 3Months
Histology(H&E stain)	(0/5)	(0/5)	(0/5)	(0/4)
MB/AR stain	(0/5)	(0/5)	(0/5)	(1/4)
Micro-CT	(0/5)	(0/5)	(0/5)	(1/4)
X-ray	(0/10)	(0/10)	(0/10)	(1/8)

Results for two months and three months for 40% defects are depicted visually in **Figures 8-15**.

Table 3: Regeneration across segment defects of 50%. MB/AR indicates that the samples were first stained with methylene blue and photographed, then stained with alizarin red and photographed. In this data set, there were 10 specimens at each time point. All specimens were first imaged by X-ray. Five of the 10 specimens were then subjected to micro CT and then MB/AR staining. The remaining 5 specimens were sectioned for H & E staining.

Assay	50% Segment defect- 15Day	50% Segment defect - 1Month	50% Segment defect - 2Months	50% Segment defect - 3Months
Histology(H&E stain)	(0/5)	(0/5)	(0/5)	0/5
MB/AR stain	(0/5)	(0/5)	(0/5)	0/5
Micro-CT	(0/5)	(0/5)	(0/5)	0/5
X-ray	(0/10)	(0/10)	(0/10)	0/10

Figures 16-22 are images of 50% defects at two and three-months post-operation.

The X-ray, micro CT and methylene blue/alizarin red data show clearly that none of the specimens with 40% segment defects at two months post-operation regenerated across the gap, and that 7/8 (87.5%) specimens at 90 days post-operation failed to regenerate cartilage. Longitudinal sections stained with H & E showed that the defect is filled in with fibrous soft tissue. None of the 50% defects had regenerated skeletal tissue even after three months. We are maintaining several animals with 40% and 50% defects for 180 days to determine whether a longer time frame will result in additional cases of skeletal regeneration, but do not expect this to happen. Regeneration across one of the 40% defects after 90 days is most likely due to posterior bending of the hind limb, which would decrease the defect length to bring the ends of the fibula close enough together for bridging. The presence of a scaffold in the CSD should inhibit bending and result in a zero incidence of regeneration for both 40% and 50% defects.

We conclude from this data that the CSD, defined in the literature as the defect length at which over 50% of the cases fail to regenerate, is somewhat less than 40%, comparable to what we found in a previous paper on CSD regeneration of the tarsus in *Xenopus laevis* hind limbs (2). Our experiments with scaffolds and growth factor delivery, however, will use a 50% defect to insure adequate challenge for regeneration.

3. Effects of Scaffolds Alone on CSD Repair

We tested the physical properties of braided pig small intestine submucosa (SIS) threads as a standard delivery scaffold. Our objective was to use the simplest biodegradable scaffold possible as a delivery vehicle for growth factors that will initiate the whole cascade of molecular and cellular events that lead to chondrogenesis and osteogenesis. We found that the dry braid scaffold should be approximately one-half the diameter of the fibula; it will swell when hydrated to the diameter of the fibula. We also found that the braid scaffold sometimes tended to unwind into separate strands when hydrated. Coating the scaffold with 5% gelatin to stiffen the braid prevented unwinding. **Figure 23** shows uncoated and gelatin-coated SIS scaffolds. **Figure 24** illustrates the insertion of a SIS scaffold into a 50% CSD. The animals do not eject the scaffolds and the gelatin-coated scaffolds stabilize the cut ends of the bone to prevent bending of the lower hind limb.

We have done a series of animals with the SIS/gelatin scaffold implanted into 50% fibula defects to determine whether the scaffold alone will foster any cell in-growth and cartilage regeneration. This experiment is still in progress, but **Figures 25 and 26** show the result at one month and two months after implant, as assessed by X-ray imaging (**Figure 25**) and H&E staining (**Figure 26**). At one month, the scaffold is still visible spanning the defect in H&E sections. By two months, the scaffold is no longer

visible, suggesting that it has degraded. No cartilage was induced by the scaffold to regenerate across the defect. The defect is filled by connective tissue and disorganized muscle fibers.

4. Absorption and release kinetics of BSA from SIS scaffolds

In anticipation of testing protein fractions of axolotl regeneration blastemas for their ability to induce cartilage regeneration across a critical size defect, we performed a protein absorption/release experiment with the different scaffolds described above. We hydrated similar-sized segments of uncoated SIS braid and 5% gelatin-coated SIS scaffolds overnight in amphibian PBS (aPBS) at 4°C. Three scaffolds of each type were then transferred separately to 1mg/ml, 5mg/ml, and 25mg/ml solutions of bovine serum albumin (BSA) in aPBS. The scaffolds were allowed to absorb BSA for three hrs. at room temperature. BSA concentration of the solutions was measured after removal of the scaffolds. To measure release of the absorbed BSA, each scaffold was placed singly in an Eppendorf tube with 1 ml of aPBS. A 100 µl sample was removed from each tube at intervals over a 72 hr. period and the BSA content of the sample measured.

Figures 27-30 show the results. Both absorption and release were proportional to the BSA concentration in which the scaffolds were soaked. The amount of BSA released into the aPBS increased over 72 hr. for both uncoated and gelatin-coated SIS. Uncoated SIS absorbed and released more protein than gelatin-coated SIS, except for the 1 mg concentration beyond 24 hr, where, for unknown reasons, more BSA was released from the gelatin-coated SIS. Growth factors are present in tissues in very small quantities, so the results suggest that we could use the gelatin-coated SIS soaked in 1 mg of protein to provide a sustained release of microgram quantities of protein. The BSA at this starting concentration shows slow and low accumulation in the aPBS for 2 hr, then a rapid increase to 72 hr.

5. Optimum technique for extraction of limb proteins

To work out the best technique for extraction of limb and blastema proteins, we made extracts of whole limb tissue, including the skeletal elements. We compared several extraction methods and concluded that (1) the efficiency of the protein extraction (protein yield/µg tissue) is adequate enough for the study; (2) the highest efficiency is obtained by grinding the tissue in liquid nitrogen plus the extraction solution from RayBio company at low temperature; and (3) even when protease inhibitors are used in the extraction procedure the protein extract is degraded over time, so the best choice is to use freshly prepared extract right before incorporation into the scaffold. This fact suggests that we might also consider directly injecting fresh protein extract into the segment defect space, as well as incorporating it into a scaffold.

6. Axolotl limb tissue grafts promote CSD and Xenopus limb regeneration

We have performed two other types of experiment relevant to the current work on blastema protein extracts (funded from a source other than TATRC and under a different animal protocol). The distal two-

thirds of the fibula and tibia were removed from *Xenopus* hind limbs and a graft of axolotl limb muscle and cartilage was inserted into the resulting space. The limb was then amputated through the distal tarsus. Control limbs received no graft. In both cases, a blastema formed from the amputation surface and gave rise to a symmetrical cartilage spike. There was no regeneration of the missing parts of the tibia and fibula in the controls. However, in the hind limbs that received grafts of axolotl tissue, the graft tissue degenerated and a cartilaginous rod bridged the gap between femur and tarsus (**Figure 31**). In the second experiment, *Xenopus* hind limbs were amputated at the mid tibia/tarsus level and a tunnel made between the skin and muscle at the amputation surface with a blunt probe. Axolotl limb cartilage and muscle was then introduced into the tunnel and the amputation site injected with 20ug retinoic acid once per week for 4 weeks. The objective was to enhance regeneration by breakdown of the axolotl tissue and release of regeneration-promoting proteins and to promote asymmetry of anteroposterior patterning by RA. Controls never regenerated more than a cartilage spike. Treated limbs often regenerated two or three digit-like structures at the end of a long cartilage rod that seemed to attain the length of a normal limb (**Figure 32**). These results suggest that axolotl proteins can induce cartilage formation across a critical size defect, as well as enhance regeneration of the poorly regenerating *Xenopus* limb.

7. Other scaffold types

In anticipation of future work using the axolotl model to screen scaffold types as well as molecules to initiate CSD regeneration, we have begun examining the behavior of other scaffolds implanted into 50% defects in the fibula. Dr. Bottino has prepared a tubular polylactic acid (PLA) scaffold by electrospinning (**Figure 33**). These scaffolds are slit lengthwise and placed in the defect with their ends overlapping the ends of the cut bone (**Figure 34**). The slit is then sutured shut to restore a closed tube. We use a slit tube because it proved difficult to maneuver the ends of the tube over the ends of the bones, although we feel that this would be possible in a larger animal. The muscle and skin of the limb are then sutured to close the wound. We are not aware of any other attempt to bridge CSDs in this way and we therefore think this scaffold design and procedure may be a useful innovation. Growth factors can be delivered into the sutured tube by injection in solution or mixed in gelatin.

However, the axolotls ejected this scaffold. Since PLA scaffolds are well tolerated in mammalian models, we are repeating the experiment with scaffolds that have been soaked in aPBS for several days to remove any contaminants. In addition, we are exchanging scaffolds with colleagues at the University of Illinois Urbana-Champaign and Central Michigan University.

8. In Silico Identification of Growth Factors That Can Potentially Effect CSD Regeneration

We pursued the networks and pathways involved in cartilage differentiation by first obtaining the relevant genes and proteins from the published literature. To extract this information, keywords related to the

process of cartilage differentiation were identified and submitted to the in-house literature-mining tool BioMAP (3). BioMAP uses a multi-level approach to identify these entities:

- (i) Part-of speech (POS) tagging by Brill Tagger to identify the noun phrases from the text.
- (ii) Biological entity classification (such as genes, proteins, cell type, organism etc.) for the noun phrases by using the UMLS and other dictionaries such as LocusLink.
- (iii) Hidden Markov Models and N-gram, machine-learning methods, to identify biological entities not discovered by dictionary matching.

The information extracted by BioMAP was normalized using the protein and gene names from the UniProt database. Human Protein Reference Database (HPRD) was used to identify the growth factors and transcription factors from this gene/protein list for each keyword submitted to BioMAP (4). HPRD provides a detailed classification of proteins into 163 distinct molecular classes such as acid phosphatase, epimerase, growth factor, transcription factor etc. Following is the list of keywords submitted to BioMAP, the number of documents (in parenthesis) obtained from PubMed, and the final list of growth factors and transcription factors.

Keyword: segment defect regeneration (229 documents)

Growth factors – insulin, vegf

Transcription factor – gcf

Keyword: segment defect regeneration rat (34 documents)

Growth factors – insulin

Transcription factor – none

Keyword: bone regeneration (24743 documents)

Growth factors - gdf9, granulin, hgf, insulin, kit ligand, pap, pdgfa, thrombopoietin, transforming growth factor alpha, vegf, amphiregulin, bmp10, egf, fgf10, fgf2, fgf23, fgf3, fgf7, follistatin, fst, gdf11, gdf5, and gdf8

Transcription factors – vdr, fosb, osterix, fosl1, p53, foxf1, pax1, gata4, pax3, gcf, pax4, gli, pax6, gli2, pax7, gli3, pax9, hand1, pparg, hes1, rel, hif1a, runx1, hoxa2, serum response factor, hoxa3, six1, hoxb3, smad1, hoxb4, smad4, isl1, smad5, lef1, smad6, mef2c, sox15, ahr, mitf, sox2, arx, mll, sox6, aryl, hydrocarbon receptor, msx2, sox9, c-fos, myc, sp1, c-myb, myf5, srf, c-myc, myocardin, sry, myod, stat1, dbp, myog, stat3, ddit3, n-myc, stat5a, tbx3, e2f1, nanog, tbx5, epas1, nfatc1, tbx6, esr1, nkx2-5, tcf1, oct4, evx1, fev, olig2, clc, satb2, smad2, smad3, smad7, taz, wt1, aes, crebbp, ctbp1, dlx5, foxp3, id1, id2, id3, lhx2, menin, pax2, pc2, pgr, and rbp1

Keyword: articular cartilage regeneration (2138 documents)

Growth factors – hgf, insulin, vegf, egf, fgf2, fst, gdf5, and grn

Transcription factors - atf5, c-fos, dbp, p53, smad1, smad6, sox9, twist

Keyword: cartilage regeneration (5587 documents)

Growth factors – amphiregulin, egf, fgf10, fgf2, fgf7, follistatin, fst, gdf5, gdf8, gdf9, granulin, grn, hgf, insulin, placental growth factor, and vegf

Transcription factors - six1, smad1, smad4, smad6, sox2, sox6, sox9, sp1, stat1, tcf1, twist, atf3, atf5, c-fos, c-myc, dbp, esr1, gcf, gli, gli3, hes1, hif1a, hoxd12, msx2, myf5, nanog, oct4, osterix, p53, pax6, and pax7

MetaCore™ from GeneGO Inc. (5) was used for the pathway and network analysis. The protein lists obtained by literature mining (described above) were used to identify predominant pathways and networks. The enrichment score in MetaCore™ is calculated based on the hypergeometric distribution:

$$p\text{-value} = \frac{K!n!(N-K)!}{N!} \sum_{i=\max(r, K+n-N)}^{\min(r, K)} \frac{1}{i!(K-i)!(n-i)!(N-K-n+i)!}$$

Where N = total number of proteins and their interactions in the MetaCore database, R = number of proteins in a given list, n = total number of proteins in a given network/pathway, and r = number of proteins from the list on a given network/pathway.

The top five pathways obtained for the biological processes related to segment defect regeneration (in descending order of significance):

1. Fracture repair/healing in chondrogenesis:

Development: HGF-dependent inhibition of TGF-beta-induced epithelial to mesenchymal transformation (EMT)

Development: Role of Activin A in cell differentiation and proliferation

Development: Regulation of EMT

Development: BMP signaling

Normal and pathological TGF-beta-mediated regulation of cell proliferation

2. Cartilage regeneration:

Development: HGF-dependent inhibition of TGF-beta-induced EMT

Normal and pathological TGF-beta-mediated regulation of cell proliferation

Development: Role of Activin A in cell differentiation and proliferation

DNA damage: Brca1 as a transcription regulator

Development: TGF-beta-dependent induction of EMT via SMADs

3. Bone regeneration:

Development: Regulation of EMT

Normal and pathological TGF-beta-mediated regulation of cell proliferation

Development: Role of Activin A in cell differentiation and proliferation

DNA damage: Brca1 as a transcription regulator

Development: HGF-dependent inhibition of TGF-beta-induced EMT

Figures 35-37 illustrate the top pathways for fracture repair, cartilage regeneration, and bone regeneration.

Figures 38-40 illustrate protein networks for fracture repair, cartilage regeneration, and bone regeneration.

Important transcription factors in the networks obtained are listed below:

1. Fracture repair/healing in chondrogenesis:

SMAD1, NANOG, c-Jun, Lef-1, Oct-3/4

2. Cartilage regeneration:

TWIST1, PAX6, STAT1, SMAD4, c-Fos

3. Bone regeneration:

NANOG, MEF2C, SRF, Oct-3/4, ID1

The pathways identified above for biological processes related to cartilage regeneration were further analyzed using several topological parameters. For each of the three groups, fracture repair/healing, cartilage regeneration, and bone regeneration, the proteins and their interactions in the top 5 pathways listed above were merged into one single file and analyzed using the CytoHubba plugin in Cytoscape (6). Four different topological parameters were used for the evaluation so as to select the proteins that are most commonly identified as significant across different topological properties. The topological properties evaluated were: bottleneck nodes, maximal cliques (MCC), eccentricity, and maximum connected component (MNC). The topological properties evaluated were: bottleneck nodes, maximal clique cover (MCC), eccentricity, and maximum neighborhood component (MNC). These are all mathematical terms used in graph theory and their mathematical definitions can be found at (7).

The following tables show the top ten most significant transcription factors, growth factors and receptors on the network for each topological property. The BMPs 2 and 7, and TGFβ-2 and 3 growth factors and their receptors and transcription factors (SMADs) emerged as the most significant. Two other significant proteins involved in the regulation of BMP signaling are Sno-N and SMURFs. The vitamin D receptor also plays an important role in chondrogenesis.

Fracture repair / healing

Bottleneck	MCC	Eccentricity	MNC
SP1	SMAD3	TGIF	SMAD3
SMAD3	SMAD2	SMAD2	SMAD2
ERK1/2	BMP Receptor 2	SMAD3	BMP receptor 2
TGF-beta receptor type I	BMPR1B	Sno-N	SMURF1
c-Jun	SMAD1	SP1	BMPR1A
TGF-beta receptor type II	SMAD4	P27KIP1	BMPR1B
SMAD5	BMPR1A	TGF-beta receptor type I	SMAD4
BMPR1A	BMP7	SARA	BMP7
SMAD1	BMP2	VDR	BMP2
SMAD4	SP1	LHX3	SMAD6

Cartilage regeneration

Bottleneck	MCC	Eccentricity	MNC
SMAD2	SMAD3	TGF-beta receptor type I	SMAD3
SP1	SMAD2	C-Raf	SMAD2
TGF-beta receptor type I	SMAD4	TGF-beta receptor type II	SNAIL1
SMAD3	SNAIL1	TGF beta 2	SMAD4
TGF-beta receptor type II	SP1	SMURF	SLUG
Brcal	HMGA2	SarA	Lef-1
ERK1/2	Brcal	TGF beta 3	SP1
GRB2	SLUG	ERK1/2	P53
TGIF	P53	H-Ras	HMGA2
MEK2	C Myc	MEK2	C-Myc

Bone regeneration

Bottleneck	MCC	Eccentricity	MNC
SP1	SMAD3	TGF-beta receptor type I	SMAD3
SMAD2	SMAD2	SARA	SMAD2
ERK1	Brcal	ERK1/2	P53
TGF-beta receptor type I	SP1	C-Raf1	SMAD4
TGF-beta receptor type II	P53	H-Ras	C-Myc
TGIF	SMAD4	SMAD2	TGF-beta receptor type I
Brcal	C-Myc	SMAD3	SARA
C-Jun	TGF-beta receptor type I	SMURF	Shc
SMAD3	SNAIL1	VDR	GRB2
Vimentin	ALK-4	TGIF	P21

Our goal was to identify the growth factors in addition to BMPs and TGF- β 2, 3 that signal these receptors to activate the transcription factors (primarily SMADs) that carry out their respective biological processes. Network connectivity was evaluated to identify such growth factors. **Figures 41-43** illustrate the Cytoscape network for the topological parameters of chondrogenesis in fracture repair, cartilage regeneration, and bone regeneration. These growth factors are listed in the Table below:

Fracture repair/healing	Cartilage regeneration	Bone regeneration
FGF2	PDGF-A	FGF2
PDGF-A	HGF	PDGF-A
EGF	TGF-beta3	EGF
HGF	Lefty-2	HGF
TGF-beta3	TGF-beta	TGF-beta
Lefty-2	VEGF-A	Lefty-2
Follistatin	FGF2	PDGF-B
PDGF-B		PDGF-D
PDGF-D		VEGF-A

Nine different growth factors appear in this table. Seven are implicated in cartilage regeneration. All except one have been implicated in fracture repair in previous studies, but only VEGF-A has been used to stimulate chondrogenesis in CSD regeneration in combination with BMP (2; for review, see 8); TGF- β has been shown to promote osteogenesis in CSD regeneration. HGF and PDGF accelerate fracture repair; HGF does this by facilitating the expression of BMP receptors. These factors will be tested for their ability to promote CSD chondrogenesis. Lefty-2, which is involved in left/right asymmetry during embryogenesis, has not been implicated in chondrogenesis, and so is an interesting molecule to test in this regard.

Key Research Accomplishments

- Characterized fracture repair in the fibula.
- Determined the critical size defect for the fibula.
- Determined that the SIS braid scaffold by itself does not promote regeneration across a CSD.
- Determined the absorption and release kinetics of BSA for uncoated and 5% gelatin-coated braided SIS scaffold.
- Performed two sets of experiments suggesting that proteins released by grafts of axolotl limb tissues to *Xenopus* froglet limbs promote both CSD regeneration of limb bones and epimorphic regeneration of limbs.
- Determined the most efficient method of protein extraction from axolotl limb tissue and regeneration blastemas, for delivery by scaffold into a CSD.
- Performed a bioinformatic analysis of the fracture healing, cartilage and bone regeneration, and segment defect regeneration literature to reveal important growth and transcription factors, and interactive protein pathways and networks involved in these processes that we hypothesize will initiate cartilage regeneration across a CSD.

Reportable Outcomes

N/A for this report.

Conclusion

The axolotl is an excellent model to screen growth factor combinations for their ability to promote regeneration of cartilage across a critical size defect (CSD) in a long bone. Regeneration is rapid compared to mammalian CSD experiments and even to the only other amphibian model, *Xenopus*. The CSD in the axolotl fibula is slightly less than 40% of the total length of the bone. Using 40% and 50% CSDs, we have demonstrated that there is no regeneration by three months post-operation, whereas regeneration takes place after fracture and segment defects of 10% and 20%. Gelatin-coated SIS appears to work well as a standard

scaffold to deliver growth factors to the segment defect space. The scaffold does not by itself promote cartilage regeneration. Release kinetic experiments indicate that protein (BSA) release from the scaffold is continuous over a period of at least 72 hr. Bioinformatic analysis has identified several growth factors that have been implicated in fracture repair but not tested for segment defect regeneration, and one protein that has not been implicated in either bone development or fracture repair.

So what does the development of this model mean for the basic science of regeneration and potential clinical application? The model offers an inexpensive alternative to the usual mammalian models that is easier to use. This means one can study events of regeneration and screen molecules and scaffolds that affect this regeneration more rapidly than the conventional models. These focus of these studies on growth factors that initiate cartilage template regeneration more realistically mimic the way endochondral bone actually develops and repairs after fracture. The model also offers the opportunity to directly compare the kind of regeneration characteristic of amputated axolotl limbs with the lack of regeneration across a CSD in the absence of any intervention, as well as with the regeneration that takes place with intervention. Understanding how to deliver growth factors that initiate cartilage regeneration from a scaffold along the length of a CSD offers the opportunity to translate these methods to mammalian models and ultimately to humans.

References

1. Song F., et al., *Organogenesis* **6**, 141 (2010).
2. Feng L., et al., *Tiss Eng A* **17**, 691 (2011).
3. Palakal M., et al., *Proc IEEE Comput Soc Bioinform Conf* **1**, 97 (2002).
4. Keshava Prasad T.S., et al., *Nucleic Acids Res.* **37**, D767 (2009).
5. Elkins S., et al., *Methods Mol. Biol.* **356**, 319 (2007).
6. Killcoyne S et al., *Methods Mol Biol* **563**, 219 (2009).
7. **Cyto-HUBBA** [<http://hub.iis.sinica.edu.tw/cytoHubba/supplementary/index.htm>]
8. Stocum D.L., *Regenerative Biology and Medicine*, 2nd ed., p. 368 (2012)

Appendix

None

Supporting Data

1. Figure Legends

Figure 1: The axolotl (*Ambystoma mexicanum*). The axolotl is neotenuous, attaining sexual maturity and living out its life in the water as an adult larva with gills. Many mutations have been discovered and bred. Clockwise from the top: Gold albino, white, eyeless, wild-type (greenish black in color), and white albino. Axolotls have enormous powers of limb, tail, and jaw regeneration but are just like mammals in their inability to regenerate bone and muscle across critical size defects.

Figure 2: Fracture gap in the mid-fibula of the axolotl hindlimb, made with scissors.

Figure 3: X-ray images of fractured axolotl fibulae. The fracture gap is indicated by the arrow in the far-right specimen.

Figure 4: Fracture repair. Left, specimen one month post-fracture, H&E stained longitudinal section. The red arrow indicates cartilage bridging the gap. The gap appears wide because the section is toward the periphery of the gap, and the new cartilage overlaps the cut ends of the bone. Right, top, specimen stained with methylene blue for cartilage and alizarin red for bone. Arrow indicates region of repair. Note that internally, the repair region is composed of cartilage (blue), while a bone shell has formed peripheral to the cartilage. Bottom, CT image of repair region at two months (arrow). T = tibia.

Figure 5: External measurement of total fibula length (fibula is exposed).

Figure 6: Removal of 50% length of the fibula (arrow).

Figure 7: Regeneration across a 20% segment defect 30 days after operation. H&E stain. New cartilage (arrow) is bridging the gap, the approximate edges of which are marked by red lines.

Figure 8: Top, X-ray images of hindlimbs in which a 20% segment defect was created in the mid fibula and photographed at one month post-operation. Although difficult to see, faint shadows indicate cartilage formation in the defect space, as indicated by the blue arrow. Bottom, methylene blue-stained 20% defect specimen, one month post-operation. Arrow indicates the new cartilage.

Figure 9: X-ray images of 10 limbs. No cartilage regeneration is visible in the segment defect in any of these specimens.

Figure 10: Left to right: Representative specimen subjected in succession to micro CT, methylene blue, and alizarin red. The cut ends of the fibula are capped and no cartilage has bridged the gap (arrow).

Figure 11: Longitudinal sections of two 40% defect specimens. The segment defect in the fibula (SD) has filled in with fibrous connective tissue. T = tibia.

Figure 12: X-ray photos of eight 40% defect specimens. One specimen has bridged the segment defect gap with cartilage (arrow).

Figure 13: Single case that regenerated across a 40% SD (arrow) by 3 months post-operation. Left to right, micro CT, methylene blue stain, alizarin red stain.

Figure 14: Representative specimen that failed to bridge a 40% segment defect, even though the gap was decreased by bending toward the posterior. Left to right, micro CT, methylene blue, alizarin red.

Figure 15: H&E section showing that 40% segment defect (SD) has filled with soft tissue (arrow) after three months. T = tibia; F = fibula

Figure 16: The 50% segment defect in the fibula has not been bridged in any of these 10 specimens by two months.

Figure 17: No regeneration has taken place between the ends of the fibula in this 50% defect case. Left to right: micro CT, methylene blue, alizarin red.

Figure 18: Methylene blue/alizarin red stain of 50% defects, two months post-operation. No cartilage has bridged the gap.

Figure 19: The 50% segment defect (SD) in this 40% defect specimen is filled with strands of fibrous connective tissue. T = tibia.

Figure 20: No new cartilage is seen three months after creating 50% defects in these specimens.

Figure 21: CT images of 50% defect specimens three months after operation. No regeneration is visible across the segment defect.

Figure 22: Five specimens of 50% defects, three months post-operation, methylene blue stain. No cartilage has regenerated across the gap.

Figure 23: Top: Non-coated 8-strand braided pig small intestine submucosa (SIS). Bottom: Same, coated with 5% gelatin.

Figure 24: Gelatin-coated SIS inserted into a 50% defect in the fibula. The black strand is the suture that will be used to close the wound.

Figure 25: X-ray images of 50% defect three months post-operation. No regeneration has occurred across the gap. T = tibia.

Figure 26: 50% defect at one and two months after embedding a gelatin-coated SIS scaffold. No cartilage has regenerated. In the one-month specimen, the implanted scaffold is still visible within the gap (arrow). At two months, the scaffold is largely gone, and connective tissue and muscle has regenerated into the gap.

Figure 27: BSA absorbed (in mg) by uncoated SIS braid (blue) and gelatin-coated (red) SIS braid at three different concentrations of BSA. Absorption is concentration dependent and greater in uncoated than coated SIS.

Figure 28: BSA released (in micrograms) from uncoated (blue) vs. gelatin-coated (red) SIS braid over a 72 hr. period. The scaffolds had been soaked in a 1 mg/ml of BSA.

Figure 29: BSA released (in micrograms) from uncoated (blue) vs. gelatin-coated (red) SIS braid over a 72 hr. period. The scaffolds had been soaked in a 5 mg/ml of BSA.

Figure 30: BSA released (in milligrams) from uncoated (blue) vs. gelatin-coated (red) SIS braid over a 72 hr. period. The scaffolds had been soaked in a 25 mg/ml of BSA.

Figure 31: Cartilage bridge across a 50% defect made in the distal two-thirds of a *Xenopus* froglet tibia/fibula after grafting axolotl cartilage and muscle into the gap and amputating through the distal tarsus.

Figure 32: Formation of a long, single cartilage extension with three symmetrical digit-like structures, after amputation through the tibia/fibula and grafting axolotl cartilage and muscle tissue into the limb stump, followed by weekly injections of 20 μ g of retinoic acid in DMSO for four weeks.

Figure 33: Polycaprolactone (PLA) scaffold, interior and surface views.

Figure 34: Tubular PLA scaffold implanted in a 50% segment defect. (a) Measuring the scaffold length; (b, c) The slit scaffold is inserted into the defect with the ends over the cut ends of the bone; (d, e) the slit is sutured shut; (f, g) the skin and muscle are sutured shut.

Figure 35: Top repair pathway identified using "chondrogenesis in fracture repair" or "cartilage regeneration" as terms: HGF-dependent inhibition of TGF-beta-induced epithelial to mesenchymal transformation.

Figure 36: Top cartilage regeneration pathway is similar to top fracture repair pathway.

Figure 37: Top pathway identified using term "bone regeneration": regulation of epithelial to mesenchymal transformation.

Figure 38: Fracture repair network.

Figure 39: Cartilage regeneration network.

Figure 40: Bone regeneration network.

Figure 41: Cytoscape network result for protein interactions derived for fracture repair/healing in chondrogenesis.

Figure 42: Cytoscape network result for protein interactions derived from cartilage regeneration.

Figure 43: Cytoscape network results for protein interactions derived from bone regeneration.

2. Powerpoint Figures



Figure 1

[PatientID]: DECAL TEST111811, [Access#]: DECAL TEST111811, [Name]: DECAL TEST111811, DECAL TEST111811, [Gender]: , [Time]: 2011/11/18 10:
[File]: 20111118103016, [StudyID]: , [Study]: , [Proc]: , [Position]: Ergon(Lat2) /
[Physician]: , [TechID]: , [Tech]: , [Station]: BIOPTRICS, [Institution]: NPI Biotech Research

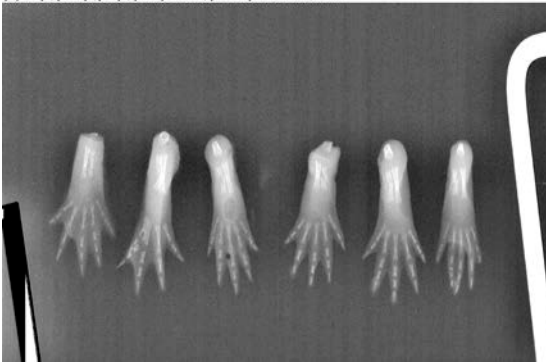


Figure 3

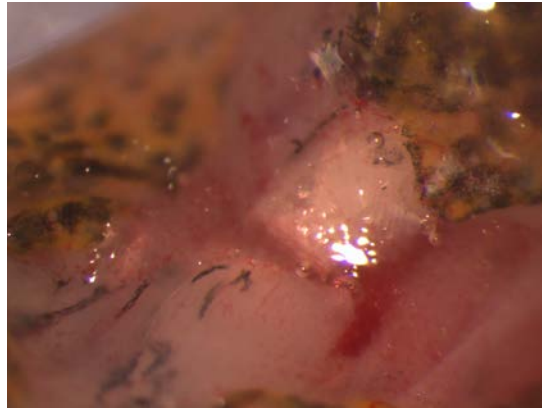


Figure 2

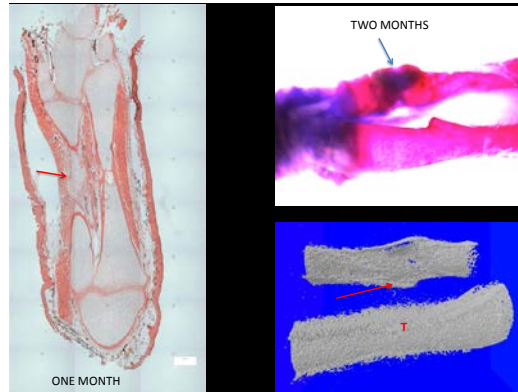


Figure 4



Figure 5

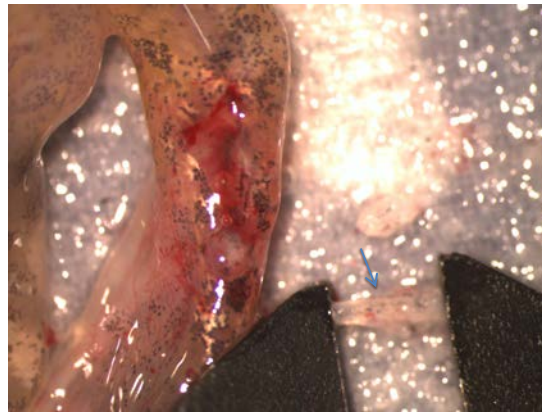


Figure 6

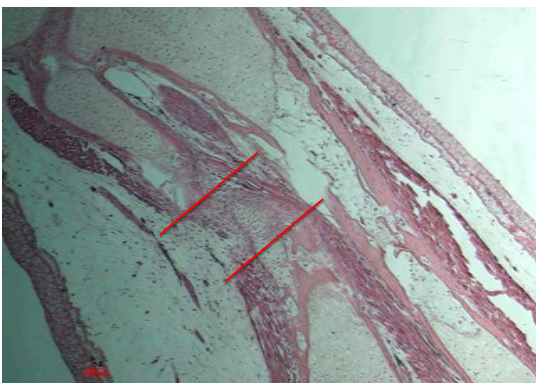


Figure 7

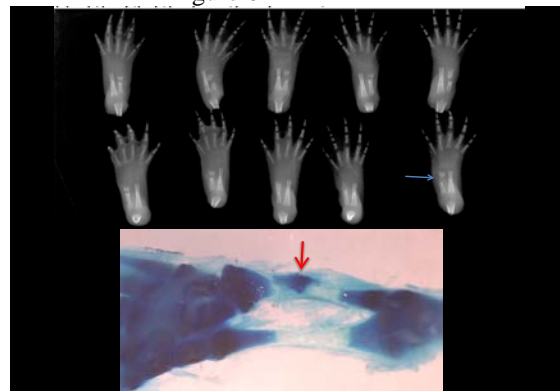


Figure 8

40% segment defect 2 months -Xray



Figure 9

40% segment defect 2 months

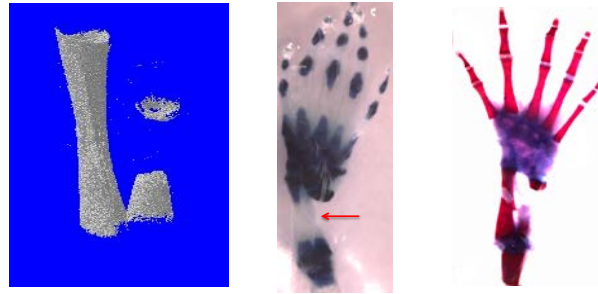


Figure 10

40% segment defect 2 months-H&E stain

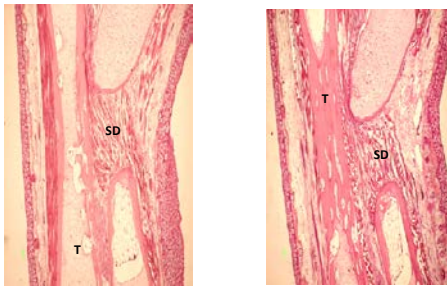


Figure 11

40% segment defect 3 months-Xray



Figure 12

40% Segment Defect—3months

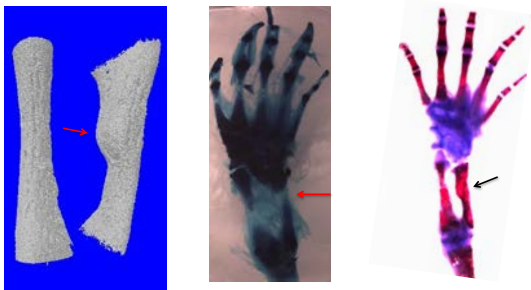


Figure 13

40% segment defect 3 months

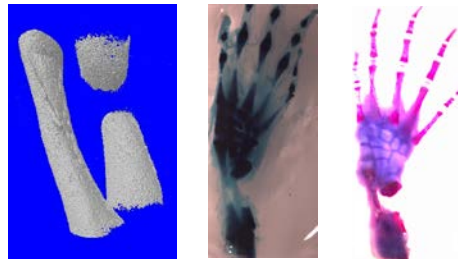


Figure 14

40% segment defect 3 months-H&E stain

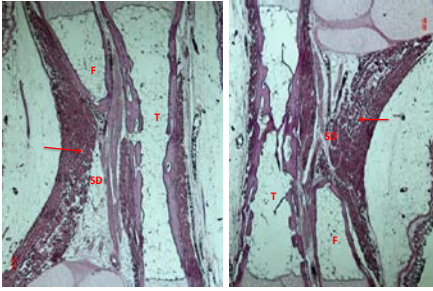


Figure 15

50% segment defect 2 months-X ray

[PatientID]: 1-10, [Access#]: 1-10, [Name]: ST0, 50%-AXOLO-2M, [Gender]: , [Time]: 2012/03/07 11:29:10
[File]: 120120307115810, [StudyID]: , [Study]: , [Proc]: , [Position]: [Organ/Lat./]
[Physician]: , [TechID]: , [Tech]: , [Station]: BIOPTICS, [Institution]: IUPUI Biotech Research



Figure 16

50% segment defect 2 months

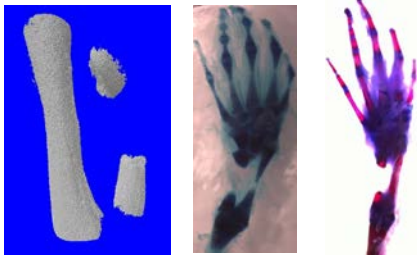


Figure 17

50% segment defect 2 months

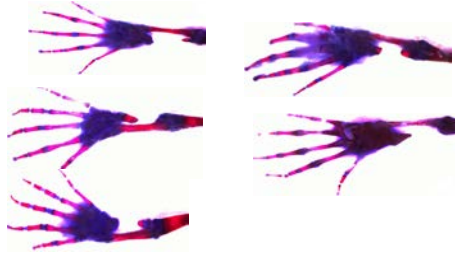


Figure 18

50% segment defect 2 months-H&E stain

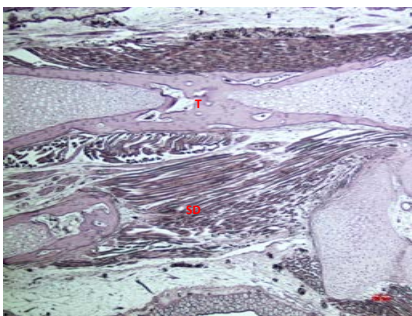


Figure 19

50% segment defect 3-month X-ray

[Access#]: 1-10, [Name]: ST0C, AXO, [Gender]: , [Time]: 2012/06/14 15:52:35
235, [StudyID]: , [Study]: , [Proc]: , [Position]: [Organ/Lat./]
D1: , [Tech]: , [Station]: BIOPTICS, [Institution]: IUPUI Biotech Research



Figure 20

50% segment defect 3-month Micro-CT

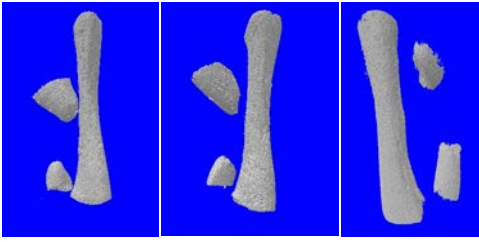


Figure 21

50% segment defect 3-month Blue stain

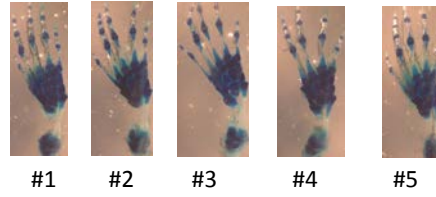


Figure 22



Figure 23

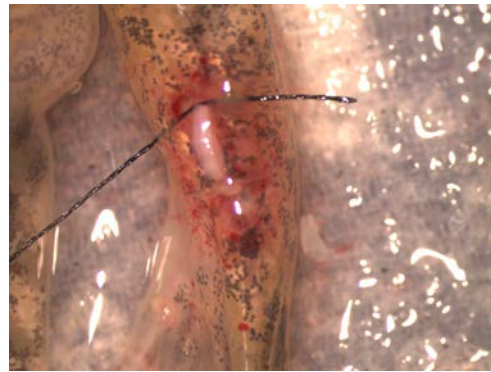


Figure 24

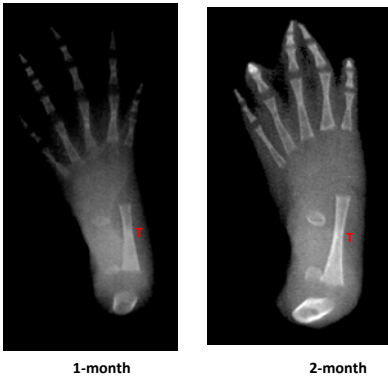


Figure 25



Figure 26

BSA Absorbed by Scaffolds

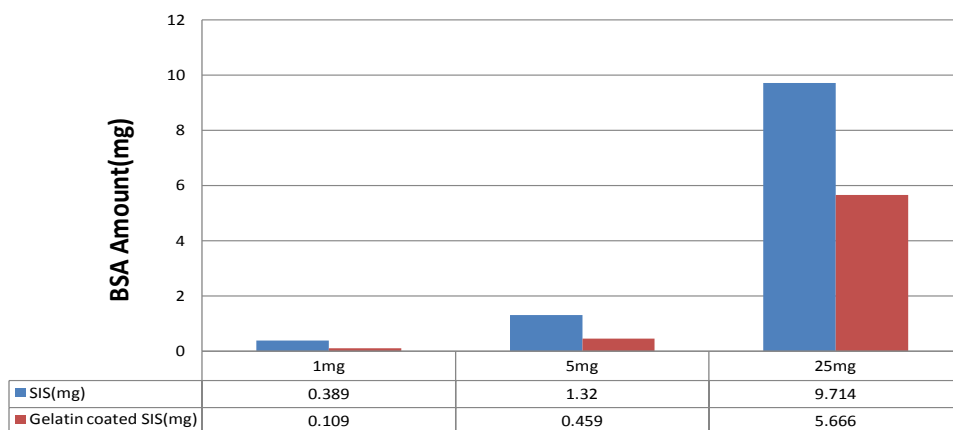


Figure 27

BSA Released by Scaffolds(1mg group)

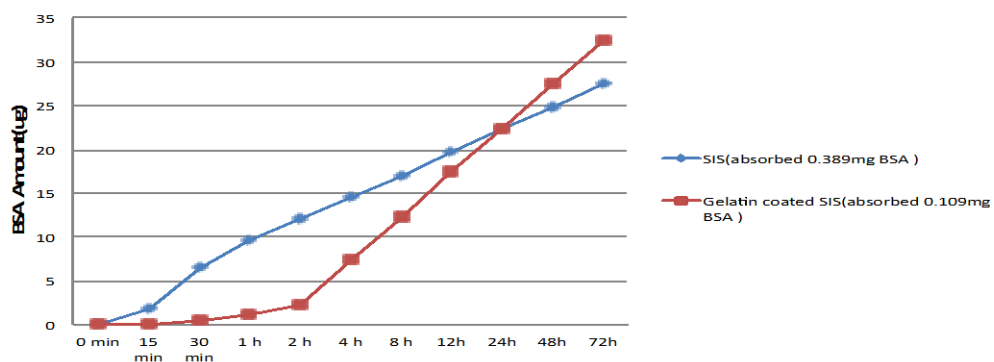


Figure 28

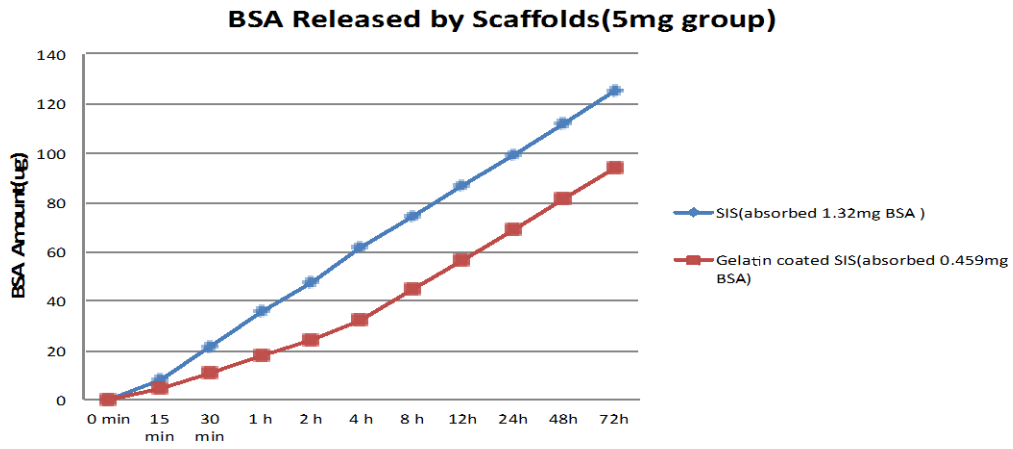


Figure 29

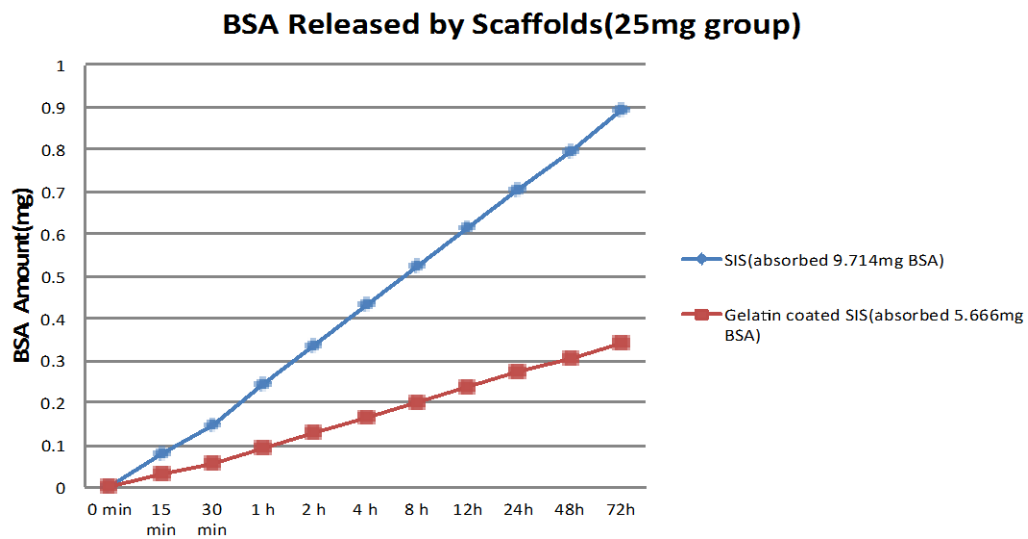


Figure 30

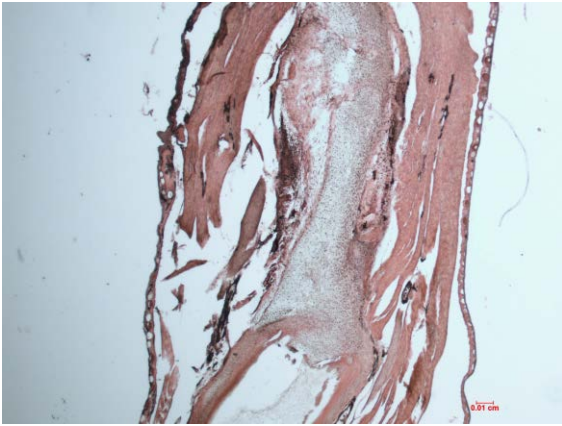


Figure 31



Figure 32

Polycaprolactone Scaffold

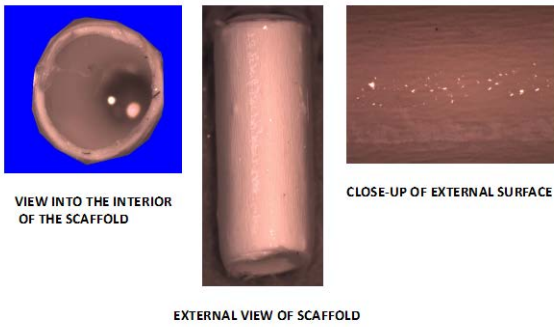


Figure 33

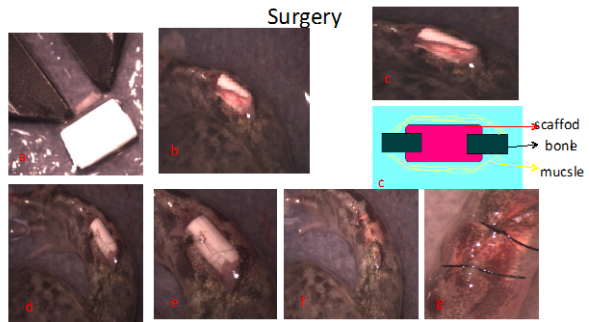


Figure 34

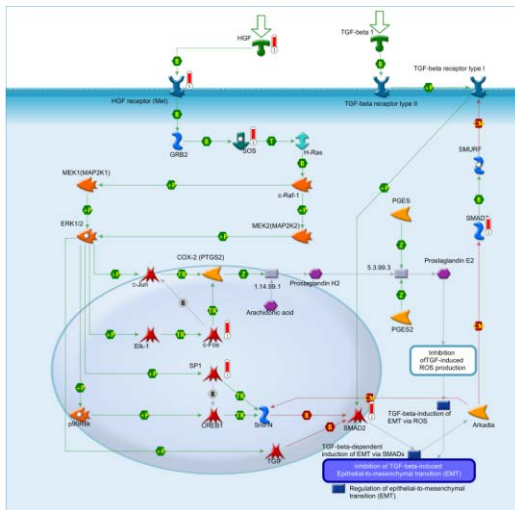


Figure 35

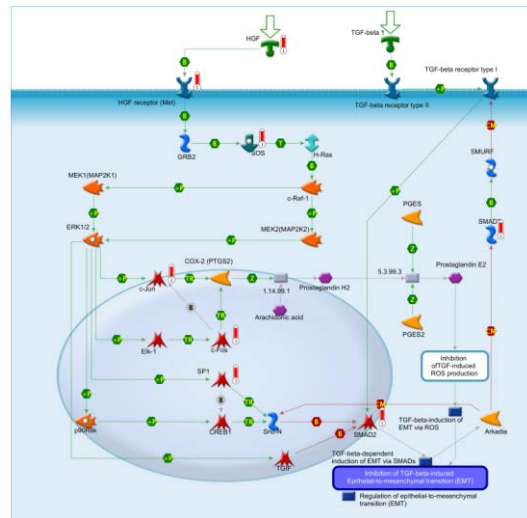


Figure 36

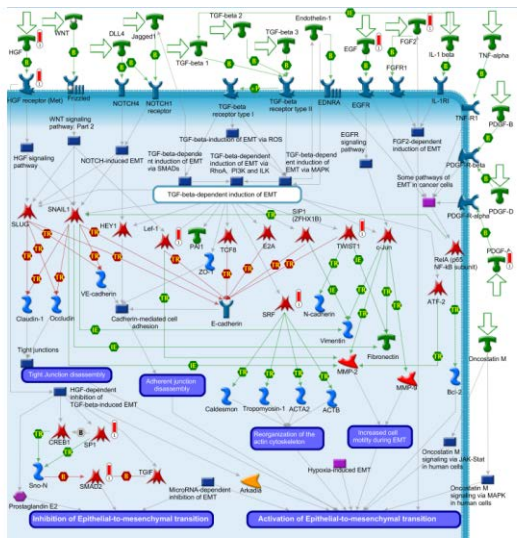


Figure 37

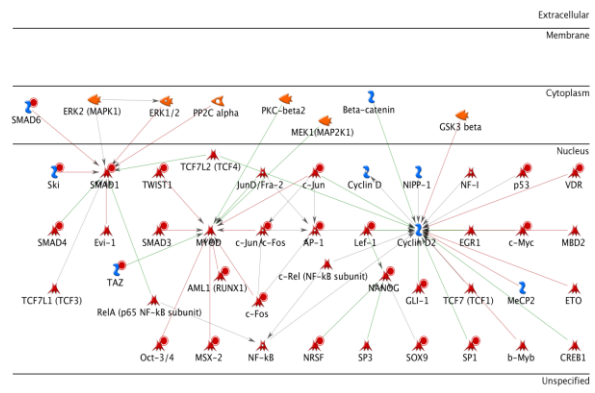


Figure 38

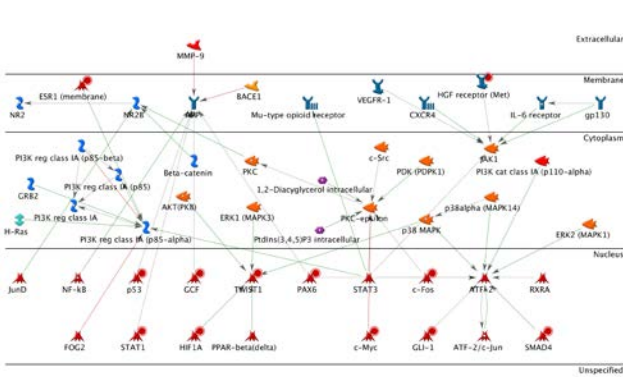


Figure 39

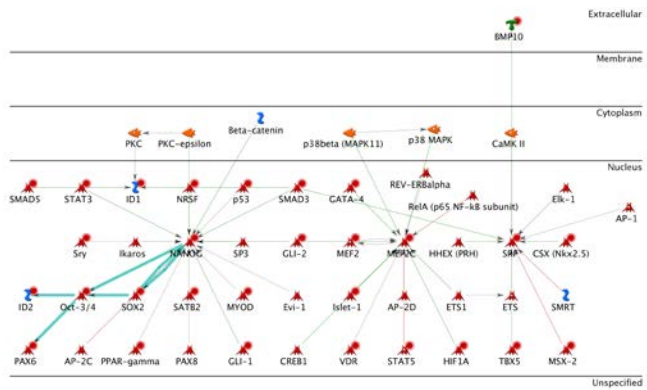
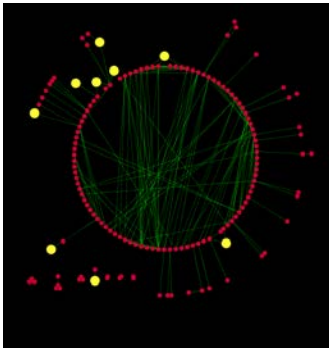


Figure 40

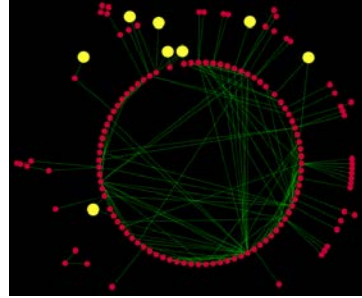
Network: Fracture repair/healing in chondrogenesis



The Cytoscape network shows the proteins (red nodes) and their interactions obtained for fracture repair/healing in chondrogenesis. The highlighted yellow nodes are the growth factors (FGF2, PDGF-A, EGF, HGF, TGF-beta3, Lefty-2, Follistatin, PDGF-B, PDGF-D) identified as upstream regulators of significant transcription factors.

Figure 41

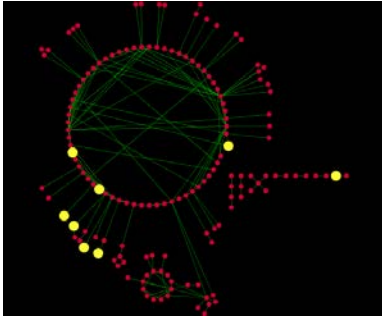
Network: Cartilage regeneration



The Cytoscape network shows the proteins (red nodes) and their interactions obtained for cartilage regeneration. The highlighted yellow nodes are the growth factors (PDGF-A, HGF, TGF-beta3, Lefty-2, TGF-beta, VEGF-A, FGF2) identified as upstream regulators of significant transcription factors.

Figure 42

Network: Bone regeneration



The Cytoscape network shows the proteins (red nodes) and their interactions obtained for bone regeneration. The highlighted yellow nodes are the growth factors (FGF2, PDGF-A, EGF, HGF, TGF-beta, Lefty-2, PDGF-B, PDGF-D, VEGF-A) identified as upstream regulators of significant transcription factors.

Figure 43